





## Research Article

# Energy Dispatching Based on an Improved PSO-ACO Algorithm

Qisong Song <sup>1</sup>, Liya Yu <sup>1</sup>, Shaobo Li <sup>2</sup>, Naohiko Hanajima <sup>3</sup>, Xingxing Zhang <sup>2</sup>,  
and Ruiqiang Pu <sup>1</sup>

<sup>1</sup>School of Mechanical Engineering, Guizhou University, Guiyang 550025, Guizhou, China

<sup>2</sup>State Key Laboratory of Public Big Data, Guizhou University, Guiyang 550025, Guizhou, China

<sup>3</sup>College of Design and Manufacturing Technology, Muroran Institute of Technology, Muroran 050-8585, Hokkaido, Japan

Correspondence should be addressed to Liya Yu; lyyu@gzu.edu.cn

Received 1 December 2022; Revised 17 January 2023; Accepted 25 January 2023; Published 20 February 2023

Academic Editor: Vasudevan Rajamohan

Copyright © 2023 Qisong Song et al. This is an open access article distributed under the Creative Commons Attribution License, which permits unrestricted use, distribution, and reproduction in any medium, provided the original work is properly cited.

In order to improve the comprehensive performance of energy dispatching between different sites, the optimization research of particle swarm optimization (PSO) algorithm and ant colony optimization (ACO) algorithm is carried out. We proposed a new improved PSO-ACO algorithm based on the idea of hybrid algorithm to solve the problem of poor energy dispatching efficiency between sites. First, the multiobjective performance indicators were introduced to transform the sites' energy dispatching problem into a multiobjective optimization problem. Second, the vitality factor was introduced into the PSO strategy to solve the local optimal problem, and in the PSO-ACO fusion strategy, the PSO routes were transformed into the ant colony enhancement pheromone to accelerate the accumulation speed of the ACO initial pheromone. Then, the angle guidance function was introduced into the state transition probability of the ACO strategy to improve the global search capability, and a high-quality pheromone update rule was proposed to improve the convergence speed of the algorithm. Finally, simulation experiments were carried out on the improved PSO-ACO algorithm, Min–Max Ant System (MMAS) algorithm, ACO algorithm, PSO algorithm, and PSO update algorithm in a variety of complex site scenarios. The simulation results show that the improved PSO-ACO algorithm can plan a site energy dispatching route with shorter route, less time-consuming, and higher security and realize the comprehensive and global optimization of energy dispatching.

## 1. Introduction

Energy is the foundation of sustainable development of human society. With the rapid development of the global economy, the demand for energy continues to increase, resulting in energy problems becoming important research carried out by human beings at present. With the over-exploitation of resources and environmental constraints, it is difficult for the energy-intensive development mode to meet the current demand. Therefore, energy dispatching has become the main mode of current energy utilization [1], where energy dispatching between different sites is a research hotspot in the energy field and a key technology of the Energy Internet. Realizing the interconnection of energy between different sites and building a large-scale energy network channel is the top priority of the current energy development layout [2].

Energy dispatching refers to rationally arranging dispatch routes of energy dispatch links to meet energy supply and demand matching. The efficiency of energy dispatching between different sites is low, the route is long, the cost is high, the safety performance is poor, and there is a problem of energy waste. Therefore, in energy dispatching, optimizing energy allocation, improving energy utilization, and planning a safe, shortest, and optimal energy route with minimum cost are the main goals of energy dispatching [3].

At present, many researchers have performed relevant research work in energy dispatching, including energy dispatching system [4], energy management system [5], energy control system [6], management method [7, 8], detection method [9], remote control method [10], and so on. However, there are few research studies on energy dispatching algorithms between different sites. The mainstream algorithms in current dispatching research are

mainly intelligent optimization algorithms, including genetic algorithm(GA) [11], PSO algorithm [12], ACO algorithm [13], grey wolf optimizer(GWO) algorithm [14], deep learning(DL) [15], differential evolution(DE) algorithm [16], fruit fly optimization Algorithm(FOA) algorithm [17], and so on.

Aiming at the problem of energy dispatching route cost, Ara et al. [18] proposed a self-regulating PSO algorithm to reduce energy costs in energy dispatching under the premise of ensuring time. Li et al. [19] proposed an improved new mayfly algorithm to reduce operating costs on the basis of ensuring the stability and balance of grid energy dispatch. Deng et al. [20] proposed an improved krill swarm algorithm to reduce the overall cost in energy dispatch and improve energy efficiency. Yu et al. [21] proposed a scheduling approach based on deep neural network and ACO, which can reduce the energy consumption cost of grid energy scheduling. Sahoo et al. [22] proposed an enhanced emperor penguin optimization algorithm to reduce the economic cost of renewable energy and microgrids dynamic dispatch.

Aiming at the problem of energy dispatching route security, Cao et al. [23] proposed a nondominated-sorting GWO algorithm to solve the power plant multiobjective load dispatching problem, which improves the accuracy of energy dispatching and realizes the safe distribution of energy. Bo et al. [24] proposed an ultrashort-term optimal dispatch strategy based on distributed robust optimization, which improves the efficiency and accuracy of dispatch and ensures the security and robustness in dispatch. Paul et al. [25] proposed a whale optimization technology based on quasi-oppositional to solve the problem of route conflict in energy dispatching and reduce the loss in transmission. Lei et al. [26] proposed a dynamic energy dispatching method based on deep reinforcement learning to solve the uncertainty in microgrids.

Aiming at the problem of energy dispatching route length, Chen et al. [27] proposed a new equilibrium optimization algorithm to solve the optimal energy scheduling problem, which has good global search performance and shortens the route length. Wang et al. [28] proposed an improved min-max power dispatching method which improves the smoothness of dispatching routes between two adjacent locations. Shang et al. [29] proposed an improved GA with simulated annealing, which improves the efficiency of dispatching, reduces the load of energy dispatching, and optimizes the dispatching route. Qiu et al. [30] proposed a robust optimization method driven by history correlation to solve the uncertainty problem of dispatching routes in microgrids, which improves the precision and linearization of dispatching routes.

Aiming at the problem of energy dispatching route time, Ellahi and Abbas [31] proposed a hybrid meta-heuristic approach to alleviate the energy dispatching problem of power plants, which reduces the cost reasonably and shortens the calculation time. Zeng et al. [32] proposed a multiobjective dispatch approach based on hierarchical progressive parallel NSGA-II algorithm, which speeds up the convergence speed of energy dispatching and reduces the algorithm iteration time. Li and Wang [33] proposed an

improved intensity pareto evolutionary algorithm 2 (ISPEA2) and improved nondominated sorting genetic algorithm 2 (INSGA2), which improve the accuracy of energy dispatching and reduce the dispatching time. Wang et al. [34] proposed an improved harmony search algorithm to alleviate the time series constraint problem in dispatching.

The research on the abovementioned algorithms only studies some of the problems existing in dispatching and lacks comprehensive research on dispatching problems. Therefore, we conducted a comprehensive study on the dispatching route problem.

PSO has been used to optimize the model parameters and was applied to many multiobjective optimization problems. Song et al. [35] proposed a feature selection algorithm based on mutual information bare bones PSO, which improves the ability to deal with high-dimensional feature selection problems. On this basis, they combined PSO with correlation-guided clustering to propose a new three-phase hybrid feature selection algorithm, which reduced the computational cost, improved the algorithm search speed in high-dimensional data, and effectively solved the constrained problems of evolutionary algorithms in high-dimensional data feature selection [36]. Lu et al. [37] proposed PSO integrating neutrino-like particles, which can enhance its global search ability in nonlinear constrained optimization problems and avoid premature convergence.

Ji et al. [38, 39] proposed a dual-surrogate-assisted and multisurrogate-assisted multitasking PSO, which can obtain multiple optimal solutions of expensive multimodal optimization problems at low computational cost. Ammar et al. [40] designed two new multiobjective binary PSO algorithms, which effectively solved multi-item capacitated lot-sizing problem. Zheng et al. [41] proposed a PSO algorithm based on migration learning, which effectively improves its search efficiency in the traveling salesman problem and can obtain better routes.

The single algorithm has the disadvantage of insufficient optimization. The hybrid algorithm can combine the advantages of different algorithms to achieve better optimization results. The hybrid algorithm combining the two algorithms has better convergence and stability. From the above research, it can be seen that the PSO algorithm has a simple structure and few parameter settings, which can be used to optimize model parameters and has a good effect in solving multiobjective optimization problems. ACO algorithm has strong robustness and powerful global search ability and is the mainstream algorithm for energy dispatching research.

In order to effectively solve the energy dispatching route problem, improve the accuracy and stability of the dispatching problem solution, and achieve the goal of obtaining a better route in a shorter time, we made the full use of the advantages of the two algorithms by hybridizing the PSO and ACO algorithms and designing a hybrid PSO-ACO algorithm with less time and stronger global search ability.

The main contributions of our work can be summarized as follows:

- (1) We proposed a new improved PSO-ACO algorithm based on the hybrid algorithm idea, which can be used to solve multiobjective optimization problems and can obtain safe energy dispatching routes with less time, lower energy consumption, and shorter length.
- (2) In the part of improving PSO, we introduced the vitality factor to increase the speed diversity, which solved the local optimum problem. Meanwhile, we introduced the routes generated by the improved PSO into the ACO, which solved the problem of lack of initial pheromone of ACO.
- (3) We optimized the state transition probability and pheromone update rules of the ACO, which effectively improves the algorithm's convergence speed and search quality, reduces the route search time, and achieves global optimization.

The main structure of this paper is as follows: Section 2 mainly describes the multiobjective optimization problem of energy dispatching. Section 3 mainly summarizes the basic principles of PSO and ACO. Section 4 proposes a new improved PSO-ACO algorithm and details its overall optimization process. Section 5 presents the simulation results and analyzes and discusses the results. Section 6 concludes the paper and gives recommendations for future work.

## 2. Problem Description

**2.1. Mathematical Modelling.** Energy dispatching between different sites is a multiobjective optimization problem, which needs to consider three aspects: route length, security, and energy consumption. We take the minimum route length, maximum security, and minimum energy consumption as the three main constraints of the multiobjective optimization problem and establish the mathematical model of the energy dispatching function.

We set the number of sites to be  $n$ ,  $N$  is the set of all sites,  $N = \{1, \dots, n\}$ ,  $i$  represent the current site,  $k$  is the previous site of site  $i$ , and  $j$  is the next site of site  $i$ .

The route length directly affects the time and efficiency of energy dispatch, the minimum route length can be described as follows:

$$\min D = \sum_{i=1}^{n-1} \sqrt{(x_j - x_i)^2 + (y_j - y_i)^2}, \quad (1)$$

where  $(x_i, y_i)$  is the site coordinate value and  $D$  is the route length.

The route security can ensure that the route of energy dispatching between different sites do not collide, maximum security can be described as follows:

$$\max S = \frac{\sum_{i=2}^{n-1} \sqrt{(x_o - x_i)^2 + (y_o - y_i)^2}}{N_r}, \quad (2)$$

where  $S$  is the route security,  $(x_o, y_o)$  is the coordinate value of the collision-prone location near the two sites, and  $N_r$  is

the number of grids passing through the dangerous area in the route.

The energy consumption can ensure that the energy dispatching can obtain a smoother route as much as possible, and the turning angle variable and turning times are taken as the main factors of the energy consumption index, and minimum energy consumption can be described as follows:

$$\min E = \mu_1 \sum_{i=2}^{n-1} \sigma(l_k, l_i) + \mu_2 N_t, \quad (3)$$

$$\sigma(l_k, l_i) = \left| \operatorname{atan} \left[ \frac{y_j - y_i}{x_{i+1} - x_i} \right] - \operatorname{atan} \left[ \frac{y_i - y_k}{x_i - x_k} \right] \right| * \frac{180}{P_i}, \quad (4)$$

where  $E$  is the energy consumption value,  $\sigma(l_k, l_i)$  is the turning angle variable between line  $l_k$  and line  $l_i$ ,  $N_t$  is the turning times, and  $\mu_1$  and  $\mu_2$  are the weight coefficient of the turning angle variable and the turning times, respectively.

In actual energy dispatching, the abovementioned evaluation indicators may lead to conflicts in the route optimization of energy dispatching. Therefore, in the route optimization of energy dispatching, it is necessary to balance various evaluation indicators, so it is necessary to set the corresponding weight coefficients for each evaluation indicator. The comprehensive multiobjective function for energy dispatching optimization can be defined as a weighted combination of minimum route length, maximum security, and minimum energy consumption, which can be described as follows:

$$J = h_D * \min D + \frac{h_S}{\max S} + h_E * \min E, \quad (5)$$

where  $h_D$ ,  $h_S$ , and  $h_E$  are the weight coefficients of the minimum route length, maximum security, and minimum energy consumption indicators, respectively.

**2.2. Basic Constraints.** In addition to the abovementioned three main constraints, there are also some basic constraints in the process of energy dispatching between different sites. These constraints include traffic balance constraint, flow direction unique constraint, and site unique constraint.

The traffic balance constraint means that the traffic arriving at site  $i$  is equal to the traffic leaving site  $i$ , which can be described as follows:

$$\sum_{k \in N, i \neq k} X_{ki} - \sum_{j \in N, j \neq i} X_{ij} = 0, i \in N, \quad (6)$$

where  $N$  is the set of all sites,  $k$  is the previous site of site  $i$ ,  $j$  is the next site of site  $i$ ,  $X_{ki}$  is the traffic arriving at site  $i$ , and  $X_{ij}$  is the traffic leaving site  $i$ .

The flow direction unique constraint means that all energies leaving site  $i$  and arriving at site  $j$  are unique, which can be described as follows:

$$\sum_{i \in N, j \neq i} X_{ij}^E = \sum_{j \in N} y_j^E, \quad (7)$$

where  $X_{ij}^E$  is the energy leaving the site  $i$ , and  $y_j^E$  is the energy arriving at the site  $j$ .

The site's unique constraint means that any station has and only one route can pass through it, which can be described as follows:

$$\sum_{k \neq i \neq j} X_{kij} = 1, k, i, j \in N, \quad (8)$$

where  $X_{kij}$  refers to the route through site  $i$ .

### 3. Intelligent Optimization Algorithm

**3.1. PSO Algorithm.** PSO algorithm is an evolutionary computing technology that simulates bird flock foraging; it seeks the optimal solution through cooperation and information sharing among individuals in the group. The particles in the PSO only have two attributes: speed and position, where speed represents the speed of movement, and position represents the direction of movement. Each particle searches for the optimal solution individually in the search space, which is marked as the individual optimal value of the particle. The individual optimal values of each particle in the particle swarm are shared with each other, and the optimal individual optimal value is found from it, which is marked as the global optimal value. Each particle in the particle swarm adjusts the next speed and position according to the global optimal value and its own particle individual optimal value.

The main process of the PSO is as follows:

- Step 1. Initialize parameters and randomly generate a batch of uniformly distributed initial particles
- Step 2. Calculate the fitness value of each particle in the population
- Step 3. Find out the individual optimal solution and the global optimal solution
- Step 4. Use the speed and position update equations to update the population
- Step 5. Determine whether the termination conditions are met. If the conditions are met, execute Step 6, otherwise, repeat Steps 2–5
- Step 6. Output the route

**3.2. ACO Algorithm.** ACO algorithm is a probabilistic algorithm that simulates ants' foraging behavior to find optimal routes. The working mechanism of the ant colony algorithm is as follows: first, we release the pheromone on the route; second, we select a route randomly in the feasible area, then accumulate the pheromone concentration through the route cycle; and finally, we select the route with the highest pheromone concentration as the target route. The main shortcomings of the ACO at this stage are insufficient initial pheromone, poor global search ability, low algorithm solution efficiency, and poor convergence. In view of the abovementioned shortcomings, the main optimization directions for improving the ACO are structure optimization, parameter optimization, multialgorithm fusion,

search strategy, pheromone initialization, and update strategy.

The main process of the ACO are as follows:

- Step 1. Initialize pheromone and related parameters;
- Step 2. Build the solution according to the state transition;
- Step 3. Update the pheromone according to the update rules;
- Step 4. Determine whether the termination condition is met. If the condition is met, execute Step 5, otherwise, repeat Steps 2–4;
- Step 5. Output the route.

### 4. Improved PSO-ACO Algorithm

**4.1. Improved PSO Strategy.** The core of PSO is to update the population using the speed and position update functions. The PSO speed update function can be described as follows:

$$v_t = \omega \cdot v_{t-1} + c_1 \cdot r_1 \cdot (p_{t-1} - x_{t-1}) + c_2 \cdot r_2 \cdot (g_{t-1} - x_{t-1}), \quad (9)$$

where  $\omega$  is the inertia weight coefficient,  $p_{t-1}$  is the particle individual optimal at the previous moment,  $g_{t-1}$  is the particle swarm global optimal at the previous moment,  $c_1$  is the current optimal learning factor,  $c_2$  is the global optimal learning factor, and  $r_1$  and  $r_2$  are random factors with a range of (0, 1).

The PSO uses linearly decreasing inertia weight coefficient, which can be described as follows:

$$\omega = \omega_{\max} - (\omega_{\max} - \omega_{\min}) \cdot \frac{T}{T_{\max}}, \quad (10)$$

where  $\omega_{\max}$  is the maximum inertia weight coefficient,  $\omega_{\min}$  is the minimum inertia weight coefficient,  $T$  is the current iteration, and  $T_{\max}$  is the maximum iterations.

In the optimization process of the PSO, with the continuous evolution of the particle swarm, the vitality of the particles continues to decline, which makes the particle speed continue to decrease, and it is easy to fall into the local optimal problem. In order to avoid the PSO falling into the local optimal problem, the vitality factor is introduced into the speed update function, which strengthens the diversity of particle optimization and expands the particle search range. The vitality factor is the particle information with the most obvious change between the global optimal solution at the current moment and the global optimal solution at the previous moment.

The improved PSO speed update function can be described as follows:

$$v'_t = \omega' \cdot v'_{t-1} + c_1 \cdot r_1 \cdot (p_{t-1} - x'_{t-1}) + c_2 \cdot r_2 \cdot (g_{t-1} - x'_{t-1}) + c_3 \cdot r_3 \cdot (k_{t-1} - x'_{t-1}), \quad (11)$$

where  $v_t'$  represents the particle velocity at the current moment,  $v_{t-1}'$  represents the particle velocity at the previous moment,  $c_3$  represents the vitality factor,  $r_3$  is the random factor with a range of (0, 1), and  $k_{t-1}$  is the particle changes, which is the most obvious change at the previous moment.

The improved PSO position update function can be described as follows :

$$x_t' = x_{t-1}' + v_t', \quad (12)$$

where  $x_t'$  is the particle position at the current moment and  $x_{t-1}'$  is the particle position at the previous moment.

The inertia weight coefficient is the core parameter to balance the global search and local search capabilities of PSO. The adaptive strategy can automatically adjust the size of the inertia weight coefficient, so that all particles in the particle swarm can continuously find the optimal solution according to certain rules and optimize the performance of the PSO. The adaptive inertia weight coefficient can be described as follows:

$$\omega' = \omega_{\max} - (\omega_{\max} - \omega_{\min}) \cdot \frac{f_i(T) - f_w}{f_b - f_w}, \quad (13)$$

where  $f_i(T)$  is the particle fitness at the  $T$ -th iteration, and  $f_b$  and  $f_w$  are the optimal and the worst value of the particle fitness at the  $T$ -th iteration, respectively.

By introducing the vitality factor and the adaptive inertia weight coefficient, the speed and position update functions of the PSO can be effectively improved, and then, the population update can be realized. In addition, the improved PSO does not just output an optimal route, but outputs the final route of all particles.

The parameters in the improved PSO strategy are shown in Table 1.

**4.2. PSO-ACO Fusion Strategy.** The pheromone accumulation of ACO is a positive feedback process, so the route formed by the ant colony in the early stage will directly affect the effective decision-making in the later stage. The optimal pheromones accumulation in the early stage of ACO is slow, which greatly affects the efficiency of energy dispatching. In order to effectively and accurately complete the initial optimal pheromone accumulation, this paper proposes a PSO-ACO fusion strategy, its specific process is as follows: First, we use the PSO to complete the route planning and generate some optimized routes. Second, we convert this part of the initial optimized routes into the enhanced pheromone of the ACO. Then, we obtain the initial pheromone of the ACO according to the environmental information. Finally, we combine the initial pheromone of the ACO with the enhanced pheromone of the ACO to obtain the initial pheromone of the improved PSO-ACO. It can be described as follows:

$$\tau_{ij}' = \tau_{ij}^{\text{ACO}} + \Delta\tau_{ij}^{\text{PSO}}, \quad (14)$$

where  $\tau_{ij}'$  is the initial pheromone of the improved PSO-ACO,  $\tau_{ij}^{\text{ACO}}$  is the initial pheromone of the ACO, and

TABLE 1: Improved PSO strategy parameters.

Variables	Description
$v_t'$	Particle velocity at the current moment
$x_t'$	Particle position at the current moment
$\omega$	Adaptive inertia weight coefficient
$\omega_{\max}$	Maximum inertia weight coefficient
$\omega_{\min}$	Minimum inertia weight coefficient
$f_i(T)$	Particle fitness at the $T$ -th iteration
$p_{t-1}$	Particle individual optimal at the previous moment
$k_{t-1}$	Particle changes most obviously at the previous moment
$f_w$	Worst value of particle fitness at the $T$ -th iteration
$m_p$	Number of particles
$c_1$	Current optimal learning factor
$c_2$	Global optimal learning factor
$c_3$	Vitality factor
$T$	Current iteration
$T_{\max}$	Maximum iterations
$r_1 r_2 r_3$	Random factors
$g_{t-1}$	Particle swarm global optimal at the previous moment
$f_b$	Optimal value of particle fitness at the $T$ -th iteration

$\Delta\tau_{ij}^{\text{PSO}}$  is the ACO enhanced pheromone converted from PSO.

Through the PSO-ACO fusion strategy, the effective fusion of PSO and ACO is realized, so that the ant colony can complete the initial pheromone accumulation faster. Meanwhile, the ACO is optimized on the basis of the PSO route, which can effectively avoid the blind search problem of the ACO and improve the algorithm convergence speed and search ability.

### 4.3. Improved ACO Strategy

**4.3.1. Improved State Transition Probability.** The state transition probability of the traditional ACO adopts the roulette wheel method, and the search efficiency of the route is poor, which can be described as follows:

$$P_{ij}(t) = \begin{cases} \frac{[\tau_{ij}(t)]^\alpha \cdot [\eta_{ij}(t)]^\beta}{\sum_{j \in J(i)} [\tau_{ij}(t)]^\alpha \cdot [\eta_{ij}(t)]^\beta}, & j \in J(i), \\ 0, & \text{otherwise,} \end{cases} \quad (15)$$

where  $\tau_{ij}(t)$  is the pheromone concentration from site  $i$  to site  $j$  at time  $t$ ,  $\alpha$  is the heuristic factor,  $\beta$  is the expectation heuristic factor,  $J(i)$  is the set of optional subsequent sites for ant at the site  $i$ , and  $\eta_{ij}(t)$  is the heuristic function of the route from site  $i$  to site  $j$  at time  $t$ , which can be described as follows:

$$\eta_{ij}(t) = \frac{1}{d_{ij}}, \quad (16)$$

where  $d_{ij}$  is the distance from site  $i$  to site  $j$ .

In order to increase the diversity of route search and improve the efficiency of route search, this paper introduces the angle guidance function based on the state transition

probability of ACO. The improved state transition probability can be described as follows:

$$\mu_{ij}(t) = \frac{|y_j - y_g|}{d_{jg}} \quad (17)$$

$$P_{ij}(t) = \left[ \tau'_{ij}(t) \right]^\alpha \left[ \eta'_{ij}(t) \right]^\beta \left[ \mu_{ij}(t) \right]^\gamma \quad (18)$$

$$P'_{ij}(t) = \begin{cases} \frac{P_{ij}(t)}{\sum_{j \in J(i)} P_{ij}(t)}, & j \in J(i), \\ 0, & \text{otherwise,} \end{cases} \quad (19)$$

where  $\tau'_{ij}(t)$  is the optimized pheromone concentration from site  $i$  to site  $j$  at time  $t$ ,  $\eta'_{ij}(t)$  is the optimized heuristic function of the route from site  $i$  to site  $j$  at time  $t$ ,  $\mu_{ij}(t)$  is the angle guidance function of the route from site  $i$  to site  $j$  at time  $t$ ,  $\gamma$  is the angle guidance factor,  $y_j$  is the ordinate of the site  $j$ ,  $y_g$  is the ordinate of the nearest target site, and  $d_{jg}$  is the distance from the next feasible site to the nearest target site.

Meanwhile, in order to improve the precision of route goal search, the heuristic function is optimized, and the distance from the next feasible node to the nearest target node is introduced based on the traditional heuristic function. The optimized heuristic function can be described as follows:

$$\eta'_{ij}(t) = \frac{1}{(\lambda \cdot d_{ij} + \mu \cdot d_{jg})^2}, \quad (20)$$

where  $\lambda$  and  $\mu$  are the corresponding weight coefficients of  $d_{ij}$  and  $d_{jg}$ , respectively.

**4.3.2. Improved Pheromone Update Rules.** The pheromone update of traditional ACO includes a local pheromone update and global pheromone update. Ants will update the local pheromone concentration from  $i$ -th node to  $j$ -th node, and the global pheromone concentration will be updated when the ant colony completes one iteration. The local pheromone and global pheromone update rules can be described as follows:

$$\tau_{ij}(t) = (1 - \delta)\tau_{ij}(t) + \delta\tau_0, \delta \in (0, 1), \quad (21)$$

$$\tau_{ij}(t+1) = (1 - \rho)\tau_{ij}(t) + \Delta\tau_{ij}(t), \quad (22)$$

where  $\tau_{ij}(t)$  is the pheromone value of the route from the  $i$ -th node to the  $j$ -th node at time  $t$ ,  $\delta$  is the local pheromone volatilization rate,  $\tau_0$  is a small constant, and  $\rho$  is the global pheromone volatilization rate.

Aiming at the problem that the global optimal pheromone cannot be found in time in the global pheromone update of the ACO, we introduce the pheromones of leader ant and follower ants and propose a high-quality ant colony pheromone update rule. Its update principle is to use the leader ant's guiding ability to lead the all follower ants to

move towards each target point and to avoid blind update of global pheromones by updating only the pheromones of the route to each target point. Our high-quality pheromone update rule can make the search range of the ant colony more concentrated on the optimal route direction in the neighborhood and can effectively improve the convergence speed and search quality of the algorithm, and finally achieve global optimization. The high-quality pheromone update rules can be described as follows:

$$\tau'_{ij}(t+1) = (1 - \rho')\tau'_{ij}(t) + \Delta\tau'_{ij}(t), \quad (23)$$

$$\Delta\tau'_{ij}(t) = \sum_{L=1}^{m_L} \Delta\tau_{ij}^L(t), \quad (24)$$

$$\rho' = \xi \left( \frac{d_{sg}}{J_b} \right), \quad (25)$$

where  $\rho'$  is the adaptive pheromone volatilization rate,  $J_b$  is the optimal route multiobjective value,  $\xi$  is the adjustment coefficient, the value is less than 1, and  $d_{sg}$  is the distance from the start site to the target site.

In the early stage of the algorithm, since  $J_b$  is large and  $\rho'$  is small, the pheromone concentration difference of each route is small, this weakens the guidance function of the leader ant and improves the global search scope and calculation accuracy of the ant. As  $J_b$  gets smaller and smaller,  $\rho'$  increases rapidly, and the pheromone concentration difference of each route increases; this enhances the guiding ability of the leader ant, improves the search speed of the ant colony, and enables the algorithm to converge quickly. The optimized pheromone increment expression is as follows:

$$\Delta\tau_{ij}^L(t) = \begin{cases} \frac{Q}{W_L} + \frac{Q}{W_F}, & j \in J(i), \\ 0, & \text{others,} \end{cases} \quad (26)$$

$$W_L = aA_L + bB_L,$$

$$W_F = \sum_{F=1}^{m_F} [A_L^F + B_L^F],$$

where  $L$  represents the leader ant,  $F$  represents the follower ants, and  $W_L$  is the route comprehensive index taken by leader ant, pheromones are allocated according to the comprehensive index, the smaller the comprehensive index, the better the route.  $W_F$  is the route comprehensive index taken by follower ants,  $Q$  is pheromone intensity,  $A_L$  is the route length of leader ant,  $B_L$  is route turns number for leader ant,  $a$  and  $b$  are the adjustment factors of route length, which can be taken according to the route demand,  $A_L^F$  is the route length of follower ants in this iteration,  $B_L^F$  is route turns number for follower ants in this iteration, and  $m_F$  is the number of follower ants. The total length and turns of the route can be described as follows:

$$A_L = \sum_{i=1}^{n-1} \sqrt{(x_{i+1} - x_i)^2 + (y_{i+1} - y_i)^2}, \quad (27)$$

$$B_L = \text{turn}(s, \dots, i, j, \dots, g), \quad (28)$$

where turn represents the turning between sites.

The parameters in the improved ACO strategy are shown in Table 2.

**4.4. Improved PSO-ACO Algorithm Flow.** The main process of the improved PSO-ACO are as follows:

- Step 1. Determine the location of each site and calculate the distance between any two sites
- Step 2. Initialize the parameters of PSO
- Step 3. Meet the three basic constraints of site dispatching
- Step 4. Update the particle individual optimal and the global optimal solution
- Step 5 Update the vitality factor
- Step 6. Update particle speed and position
- Step 7. According to the three constraints of minimum route length, maximum security, and minimum energy consumption, find some routes that satisfies any one of the constraints
- Step 8. Determine whether the maximum iteration of the particle swarm is reached. If it is, execute Step 9, otherwise, repeat Steps 4–7
- Step 9. Output the optimized routes generated by the improved PSO
- Step 10. Initialize the parameters of the ACO and obtain the initial pheromone of the ant colony
- Step 11. Convert the optimized routes of PSO into ant colony enhancement pheromone
- Step 12. Obtain the initial pheromone of the improved PSO-ACO. By fusing the initial pheromone and the enhancement pheromone of the ant colony
- Step 13. Move ants using the improved state transition probability
- Step 14. Modify pheromone concentration using the improved pheromone update rules
- Step 15. Meet the three main constraints and find the optimal route
- Step 16. Determine whether the maximum iteration of the ant colony is reached. If it is, execute step 17, otherwise, repeat steps 12–15
- Step 17. Output the optimal route of the improved PSO-ACO.

The algorithm flowchart of the improved PSO-ACO algorithm is shown in Figure 1.

#### 4.5. Constraint Handling Methods and Computational Complexity

**4.5.1. Constraint Handling Methods.** There are three basic constraints and three main constraints for energy dispatching between different sites, we should strictly follow these three basic constraints and meet three main constraints when executing the algorithm.

We set three basic constraints as the premise and basic criterion for the algorithm to find the site route. If the algorithm conflicts with the three basic constraints in the process of finding routes in the early stage, it means that the routes found are not met with the constraints, and they are discarded directly.

We set three main constraints as the objective function for the algorithm to find the optimal route. In the improved PSO part, the routes found by particles with fewer violations of the main constraints are called good routes. In the improved ACO part, the route found by ants that do not violate the three main constraints is the final optimal route.

In the process of algorithm execution, first, based on the three basic constraints, we find feasible routes that meet them. Second, based on the three main constraints, we find some good routes that meet any one or more constraints. Finally, on this basis, the optimal route that fully meets the three main constraints is found.

**4.5.2. Computational Complexity.** Computational complexity is the resources occupied by the algorithm operation, mainly including time complexity and space complexity. Time complexity is how much time the algorithm takes during operation, space complexity is the size of the memory occupied by the algorithm during operation, and they are usually approximated by large  $O$  values.

We set the site number of the energy dispatching problem as  $n$ , the improved PSO-ACO algorithm mainly includes improved PSO, PSO-ACO fusion, and improved ACO. Then, the time complexity of the proposed method is the combination of the improved PSO and ACO time, which can be described as follows:

$$T(n) = O(T_{\max} * m_p * n) + O(N_{\max} * m_a * n), \quad (29)$$

where  $O(T_{\max} * m_p * n)$  represents the time complexity of the improved PSO, that is, the time complexity of all particles traversing  $n$  sites under its total number of iterations.  $O(N_{\max} * m_a * n)$  represents the time complexity of the improved ACO, that is, the time complexity of all ants traversing  $n$  sites under its total number of iterations.

The space complexity of the proposed method is the memory occupied by the data stored by the algorithm and the data generated during the operation of the algorithm, which can be described as follows:

$$S(n) = O(n^2) + O(m_p * n) + O(m_a * n) + O(n), \quad (30)$$

TABLE 2: Improved ACO strategy parameters.

Variables	Description
$\alpha$	Heuristic factor
$\beta$	Expectation heuristic factor
$\gamma$	Angle guidance factor
$\lambda$	Weight coefficients of $d_{ij}$
$\rho'$	Adaptive pheromone volatilization rate
$\xi$	Adjustment coefficient
$a, b$	Adjustment factors of route length
$m_a$	Number of ants
$F_{\max}$	Maximum iterations
$\tau_{ij}^{\text{ACO}}$	Initial pheromone of the ACO
$\Delta\tau_{ij}^{\text{PSO}}$	ACO enhanced pheromone converted from PSO
$\eta_{ij}(t)$	Optimized heuristic function of the route from site $i$ to site $j$ at time $t$
$\mu_{ij}(t)$	Angle guidance function of the route from site $i$ to site $j$ at time $t$
$d_{ij}$	Distance from site $i$ to site $j$
$d_{jg}$	Distance from site $j$ to site $g$
$d_{sg}$	Distance from site $s$ to site $g$
$\mu$	Weight coefficients of $d_{jg}$
$A_L^L$	Route length of leader ant
$A_L^F$	Route length of follower ants
$B_L^L$	Route turns number for leader ant
$B_L^F$	Route turns number for follower ants
$Q$	Pheromone intensity
$J_b$	Optimal route multiobjective value
$\tau_{ij}(t)$	Optimized pheromone concentration from site $i$ to site $j$ at time $t$
$W_L$	Route comprehensive index taken by leader ant
$W_F$	Route comprehensive index taken by follower ants

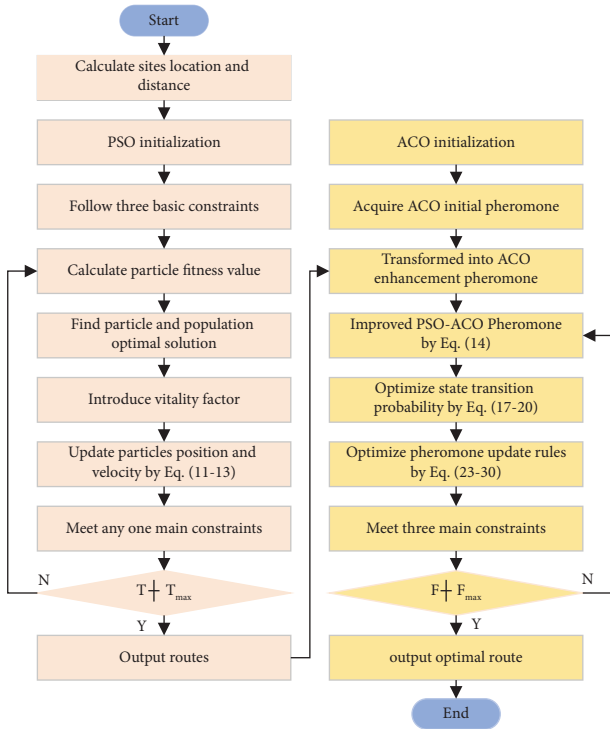


FIGURE 1: Improved PSO-ACO algorithm flowchart.

where  $O(n^2)$  represents the space complexity of storing the distance between any two sites,  $O(m_p * n)$  represents the space complexity of storing and recording the PSO route

generation,  $O(m_a * n)$  represents the space complexity of storing and recording the ACO route generation, and  $O(n)$  represents the space complexity of storing the final optimal solution.

## 5. Experimental Results and Analysis

### 5.1. Experimental Platform and Algorithm Parameter Setting

**5.1.1. Experimental Platform.** In order to verify the feasibility and effectiveness of the improved PSO-ACO algorithm proposed in this paper in energy scheduling, simulation experiments were conducted on the improved PSO-ACO algorithm, ACO algorithm, MMAS algorithm, PSO algorithm, and PSO update algorithm, respectively. The simulation environment is 20 cm  $\times$  20 cm, there are 10 sites for energy dispatching. Different locations are set for the 10 sites, which can form different experimental scenarios. The simulation experiment is based on the HP Pavilion personal computer (Intel (R) Core (TM) I7-9700F CPU, 3.0 GHz, 8 GB memory; NVIDIA Geforce GTX 1080 GPU).

**5.1.2. Improved PSO-ACO Parameter.** In the improved PSO-ACO algorithm proposed in this paper, the parameters are set as follows: the number of particles  $m_p$  is 80, maximum PSO iterations  $T_{\max}$  is 2000, current optimal learning factor  $c_1$  is 1.5, global optimal learning factor  $c_2$  is 1.5, vitality factor  $c_3$  is 2, maximum inertia weight coefficient  $\omega_{\max}$  is 0.9, minimum inertia weight coefficient  $\omega_{\min}$  is 0.3, number of ants  $m_a$  is 20, maximum ACO Iterations  $F_{\max}$  is 2000,



heuristic factor  $\alpha$  is 1, expectation heuristic factor  $\beta$  is 7, angle guidance factor  $\gamma$  is 8, weight coefficient  $\lambda$  is 1, and the other weight coefficient  $\mu$  is 3.

*5.1.3. Comparison Algorithm Parameter.* The four comparison algorithms are as follows:

ACO [42], a solution space search method suitable for finding optimal routes on graphs

MMAS [43], a search method that sets the maximum and minimum pheromone intervals and adopts elite rules

PSO [44], a solution search method based on information sharing among groups and evolving from disorder to order

PSO update [45], a PSO optimization method for constantly updating particle position and velocity

In the experiment, different parameters of the algorithm may lead to different experimental results, and the same basic parameters of the algorithm can ensure the fairness of the algorithm comparison. In principle, the four comparison algorithms and the improved PSO-ACO algorithm should be set with the same parameters as much as possible.

According to the parameters of the improved PSO-ACO algorithm, we set the parameters of ACO and MMAS as follows: the number of ants is set to 20, the maximum iterations number is set to 2000, the heuristic factor is set to 1, the expectation heuristic factor is set to 7, and the pheromone volatilization rate is set to 0.3. In addition, the lower limit of pheromone concentration of MMAS is set to 0.1, and the upper limit of pheromone concentration is 1000.

We set the parameters of PSO and PSO update as follows: The number of particles is set to 80, the maximum iterations number is set to 2000, the inertia weight coefficient is set to 0.8, the current optimal learning factor is 1.5, and the global optimal learning factor is 1.5.

For the rest of the parameters in the comparison algorithms, we adopt the default settings suggested in the corresponding literature.

## 5.2. Simulation Experiment

*5.2.1. Experimental Scenario 1.* On the premise of setting 10 sites at different locations, multiple sets of simulation experiments were carried out for the 5 algorithms, respectively. In scenario 1, the energy dispatching routes of five algorithms are shown in Figure 2.

In Figure 2, the energy dispatching route length of the improved PSO-ACO algorithm is 58.05 cm, and the coincidence point is 0. The energy dispatching route length of the MMAS algorithm is 66.57 cm, and the coincidence point is 1. The energy dispatching route length of the ACO algorithm is 71.28 cm, and the coincidence point is 2. The energy dispatching route length of the PSO update algorithm is 73.01 cm, and the coincidence point is 1. The energy

dispatching route length of the PSO algorithm is 97.63 cm, and the coincidence point is 2.

Because pheromone is unique to ACO algorithm, pheromone can only exist in ACO algorithm and its optimization algorithm, so there is no pheromone in both PSO algorithm and PSO update algorithm. Based on this, only the improved PSO-ACO algorithm, MMAS algorithm, and ACO algorithm have pheromone in the above five algorithms. The pheromone situation of the three algorithms is shown in Figure 3.

In Figure 3, the pheromone of the improved PSO-ACO algorithm is concise and clear, while the pheromone of the MMAS algorithm and the ACO algorithm is more complex.

*5.2.2. Experimental Scenario 2.* In scenario 2, the energy dispatching routes of five algorithms are shown in Figure 4.

In Figure 4, the energy dispatching route length of the improved PSO-ACO algorithm is 64.29 cm, and the coincidence point is 0. The energy dispatching route length of the MMAS algorithm is 69.09 cm, and the coincidence point is 1. The energy dispatching route length of the ACO algorithm is 76.93 cm, and the coincidence point is 2. The energy dispatching route length of the PSO update algorithm is 80.42 cm, and the coincidence point is 2. The energy dispatching route length of the PSO algorithm is 90.23 cm, and the coincidence point is 3.

The pheromone situations of the three algorithms are shown in Figure 5.

In Figure 5, the pheromone of the improved PSO-ACO algorithm is concise and clear, while the pheromone of the MMAS algorithm and the ACO algorithm is more complex.

*5.2.3. Experimental Scenario 3.* In scenario 3, the energy dispatching routes of five algorithms are shown in Figure 6.

In Figure 6, the energy dispatching route length of the improved PSO-ACO algorithm is 72.74 cm, and the coincidence point is 0. The energy dispatching route length of the MMAS algorithm is 74.21 cm, and the coincidence point is 1. The energy dispatching route length of the ACO algorithm is 84.60 cm, and the coincidence point is 2. The energy dispatching route length of the PSO update algorithm is 90.03 cm, and the coincidence point is 1. The energy dispatching route length of the PSO algorithm is 102.71 cm, and the coincidence point is 6.

The pheromone situations of the three algorithms are shown in Figure 7.

In Figure 7, the pheromone of the improved PSO-ACO algorithm is concise and clear, while the pheromone of the MMAS algorithm and the ACO algorithm are more complex.

*5.3. Simulation Results and Analysis.* In order to ensure the effectiveness of the algorithm, we set up 20 experimental scenarios and carried out 20 sets of simulation experiments on five algorithms, respectively. The experimental data are shown in Table 3.

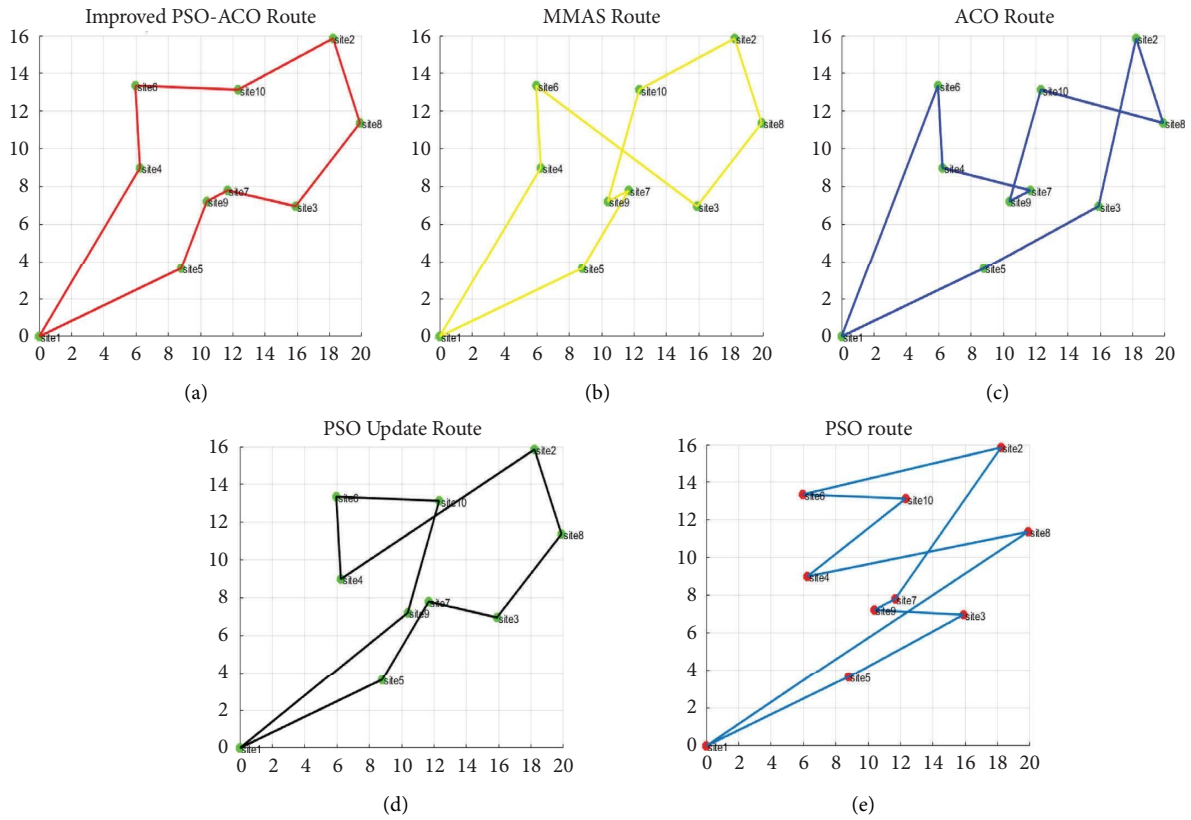


FIGURE 2: Energy dispatching routes of five algorithms in scenario 1. (a) Improved PSO-ACO algorithm energy dispatching route; (b) MMAS algorithm energy dispatching route; (c) ACO algorithm energy dispatching route; (d) PSO update algorithm energy dispatching route; (e) PSO algorithm energy dispatching route.

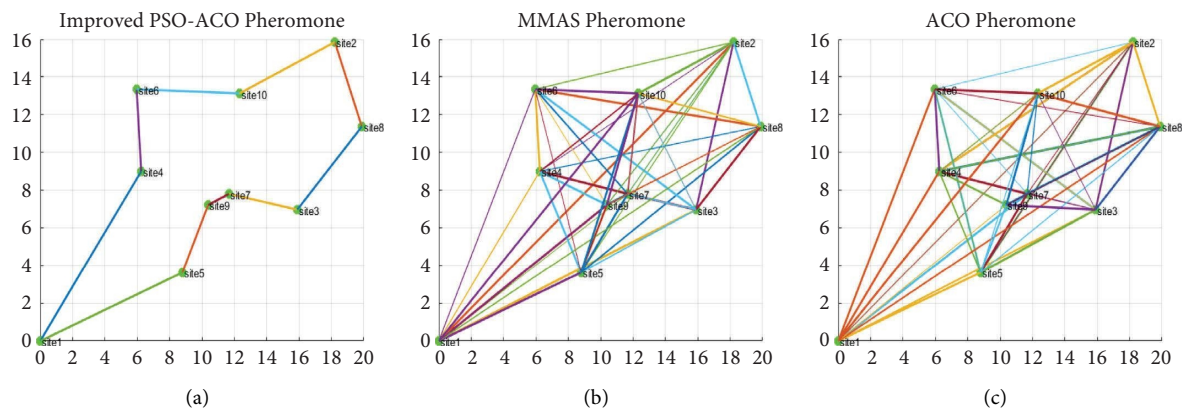


FIGURE 3: Pheromones of three algorithms in scenario 1. (a) Improved PSO-ACO algorithm phomone; (b) MMAS algorithm phomone; (c) ACO algorithm phomone.

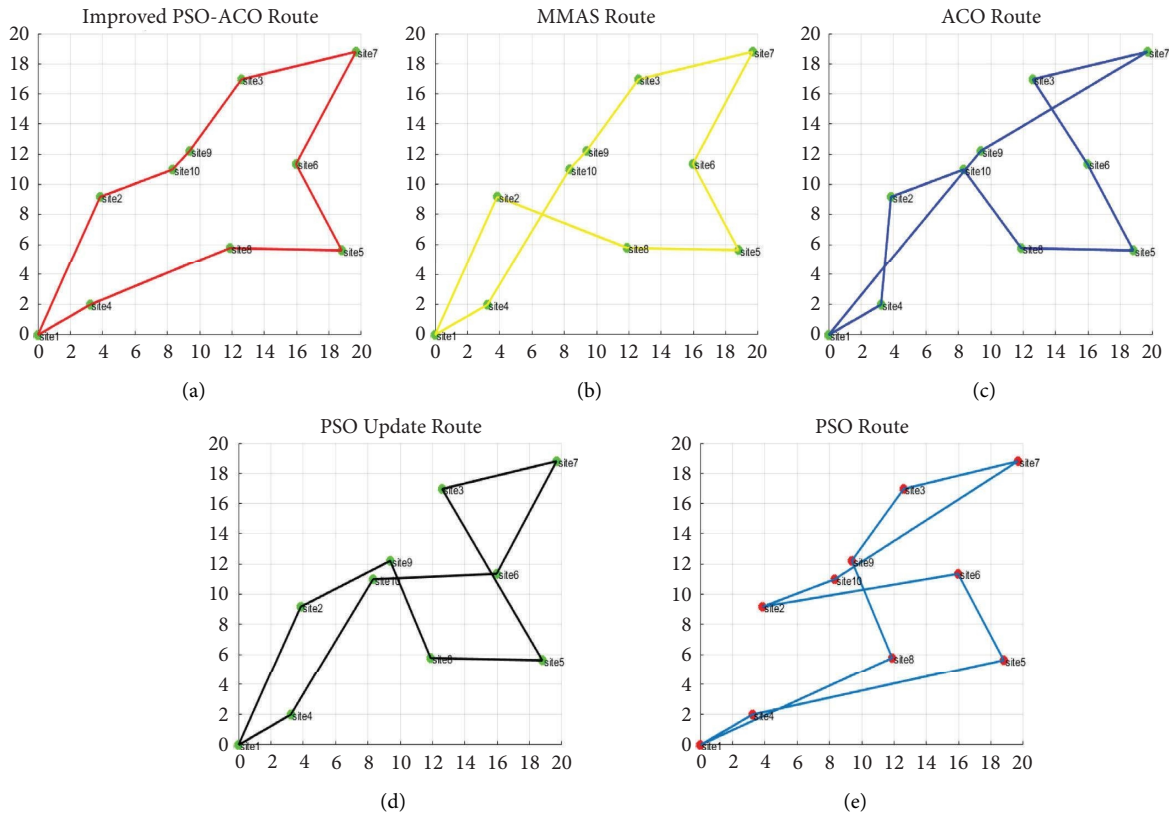


FIGURE 4: Energy dispatching routes of five algorithms in scenario 2. (a) Improved PSO-ACO algorithm energy dispatching route; (b) MMAS algorithm energy dispatching route; (c) ACO algorithm energy dispatching route; (d) PSO update algorithm energy dispatching route; (e) PSO algorithm energy dispatching route.

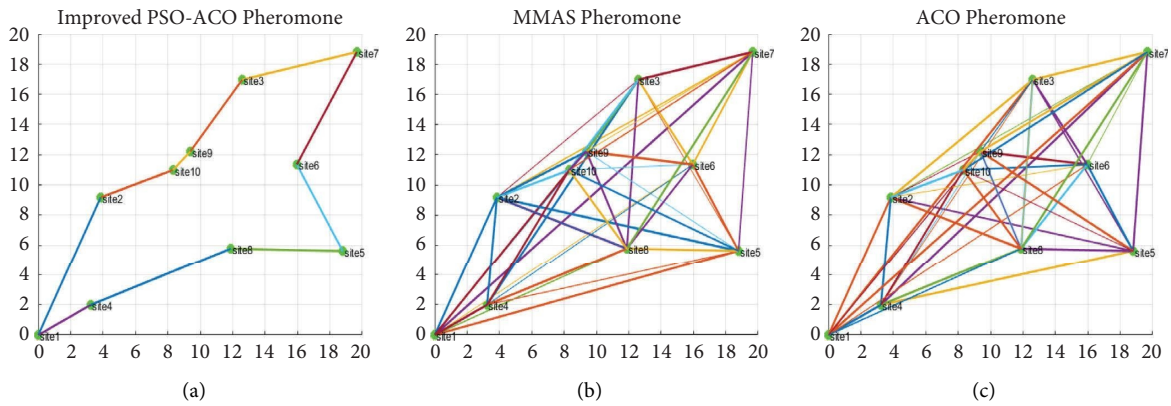


FIGURE 5: Pheromones of three algorithms in scenario 2. (a) Improved PSO-ACO algorithm pheromone; (b) MMAS algorithm pheromone; (c) ACO algorithm pheromone.

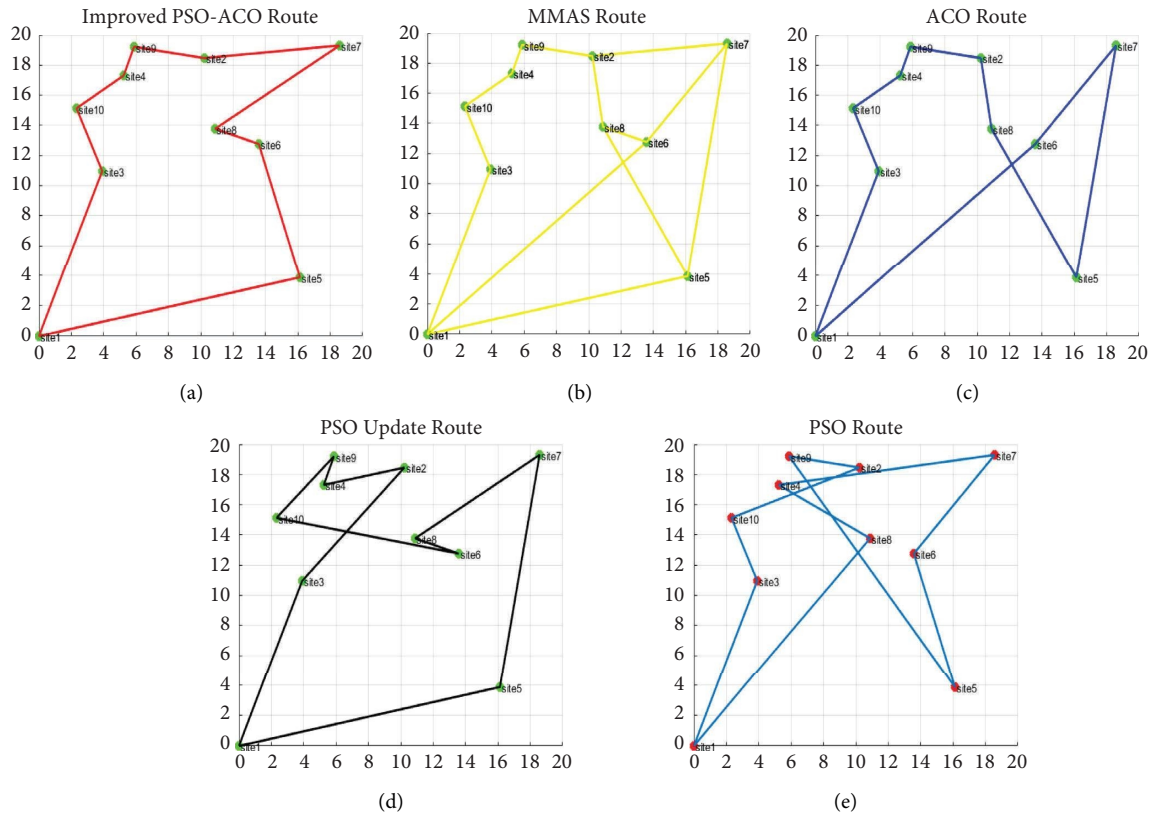


FIGURE 6: Energy dispatching routes of five algorithms in scenario 3. (a) Improved PSO-ACO algorithm energy dispatching route; (b) MMAS algorithm energy dispatching route; (c) ACO algorithm energy dispatching route; (d) PSO update algorithm energy dispatching route; (e) PSO algorithm energy dispatching route.

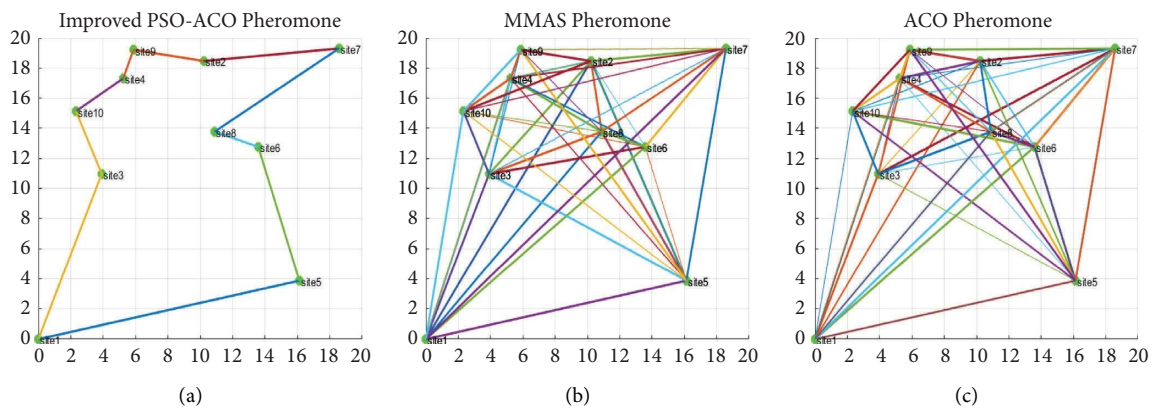


FIGURE 7: Pheromones of three algorithms in scenario 3. (a) Improved PSO-ACO algorithm pheromone; (b) MMAS algorithm pheromone; (c) ACO algorithm pheromone.

TABLE 3: Experiment results of intelligent algorithm energy dispatching.

S	IPSO-ACO			ACO			MMAS			PSO			PSO update		
	L (cm)	T (s)	P	L (cm)	T (s)	P	L (cm)	T (s)	P	L (cm)	T (s)	P	L (cm)	T (s)	P
1	58.05	2.89	0	71.28	4.73	2	66.57	3.8	1	97.63	4.75	2	73.01	3.85	1
2	64.29	3.14	0	76.93	4.42	2	69.09	3.5	1	90.23	4.87	3	80.42	4.21	2
3	72.74	3.35	0	84.60	4.55	1	74.21	3.84	1	102.71	4.67	6	90.03	3.88	1
4	63.50	3.08	0	72.76	4.5	1	70.59	3.86	0	78.89	4.94	2	70.67	4.07	1
5	78.98	3.53	0	86.17	4.65	1	82.42	3.91	0	114.15	4.68	3	100.34	4.27	2
6	62.59	2.68	0	75.19	4.16	1	65.90	3.87	1	94.50	4.54	5	78.99	3.91	2
7	64.41	3.29	0	80.08	4.27	2	72.12	3.78	1	93.58	4.63	3	84.21	4.05	2
8	58.74	2.97	0	68.90	4.23	2	60.36	3.99	1	72.15	4.35	2	68.22	3.93	1
9	61.13	2.78	0	70.73	4.12	3	67.07	3.93	1	76.29	4.12	3	70.70	3.86	2
10	64.87	2.82	0	69.71	4.06	1	68.67	3.6	1	74.93	4.76	2	71.01	3.94	1
11	79.35	2.92	0	90.43	4.94	2	81.83	3.93	1	117.45	4.64	6	95.27	3.98	1
12	66.65	3.26	0	70.79	4.38	2	67.51	3.63	1	77.23	4.84	2	70.85	3.85	2
13	62.12	3.05	0	69.49	4.03	1	65.61	3.74	0	77.11	4.59	2	70.87	3.76	1
14	64.43	3.04	0	74.05	4.28	2	70.29	3.61	1	79.98	4.96	2	71.39	4.12	1
15	75.08	3.35	0	86.86	4.64	1	77.48	3.72	0	96.66	4.67	2	85.43	4.05	1
16	66.86	2.92	0	82.24	4.43	2	70.99	3.83	1	88.03	4.79	3	82.56	4.08	0
17	61.04	3.02	0	71.98	4.13	1	65.83	3.67	0	76.83	4.92	2	73.61	4.11	1
18	60.94	2.98	0	68.55	4.11	1	63.56	3.78	1	83.26	4.99	5	79.48	4.07	2
19	62.6	3.06	0	67.69	4.09	1	63.63	3.84	0	99.51	4.93	6	68.67	3.95	2
20	72.93	3.26	0	87.80	4.24	2	79.56	3.97	1	90.80	4.91	2	80.78	4.09	1

In Table 3, S represents the sites, L represents the route length, T represents the route time, and P represents the route coincidence point.

It can be seen from Table 3 that in 20 experiments, the energy dispatching route length range of the improved PSO-ACO algorithm is from 58.05 cm to 79.35 cm, the time-consuming range is from 2.68 s to 3.53 s, and the coincidence point is always 0. The energy dispatching route length range of the MMAS algorithm is from 60.36 cm to 82.42 cm, the time-consuming range is from 3.50 s to 3.99 s, and the coincidence point is 0 or 1. The energy dispatching route length range of the ACO algorithm is from 67.69 cm to 90.43 cm, the time-consuming range is from 4.03 s to 4.94 s, and the coincidence point range is from 1 to 3. The energy dispatching route length range of the PSO update algorithm is from 68.22 cm to 100.34 cm, the time-consuming range is from 3.76 s to 4.27 s, and the coincidence point range is from 0 to 2. The energy dispatching route length range of the PSO algorithm is from 72.15 cm to 117.45 cm, the time-consuming range is from 4.12 s to 4.99 s, and the coincidence point range is from 2 to 6.

In order to better observe the experimental results, the experimental data are visualized and compared. The visualization effects of 20 experiments are shown in Figure 8.

It can be seen from Figure 8 that under 20 different energy dispatching experimental scenarios, the improved PSO-ACO algorithm has the shortest dispatching route, the least time-consuming, and no route overlap. MMAS algorithm, ACO algorithm, PSO update algorithm have longer dispatching routes, more time-consuming, and more coincidence points. PSO algorithm has the longest dispatching route, the most time-consuming, and the most coincidence points. The simulation results show that the improved PSO-ACO algorithm proposed in this paper is effective and superior in energy dispatching.

Meanwhile, according to the comprehensive performance indicators such as energy dispatching route length, route time, and route coincidence points, 20 sets of experimental data are comprehensively analyzed, and the average performance indicators of five algorithms can be obtained, as shown in Table 4.

Based on the average performance indicators of the five algorithms, the following conclusions can be reached.

- (1) In Table 4, the average route length of the improved PSO-ACO algorithm proposed in this paper in the energy dispatching simulation experiment is 66.07 cm, the average time is 3.07 s, and the average route coincidence point is 0.
- (2) It can be seen from Table 4 that the improved PSO-ACO algorithm proposed in this paper has the shortest route. The average route length is 10.24 cm, 4.09 cm, 14.03 cm, and 12.26 cm less than the ACO algorithm, MMAS algorithm, PSO algorithm, and PSO update algorithm, respectively.
- (3) It can be seen from Table 4 that the improved PSO-ACO algorithm proposed in this paper has the shortest time. The average time is 1.28 s, 0.72 s, 1.66 s, and 0.93 s less than the ACO algorithm, MMAS algorithm, PSO algorithm, and PSO update algorithm, respectively.
- (4) It can be seen from Table 4 that the improved PSO-ACO algorithm proposed in this paper has the fewest coincidence points. The average coincidence point is 1.55, 0.7, 3.15, and 1.35 less than ACO algorithm, MMAS algorithm, PSO algorithm, and PSO update algorithm respectively.
- (5) In conclusion, the improved PSO-ACO algorithm proposed in this paper is a successful multiobjective

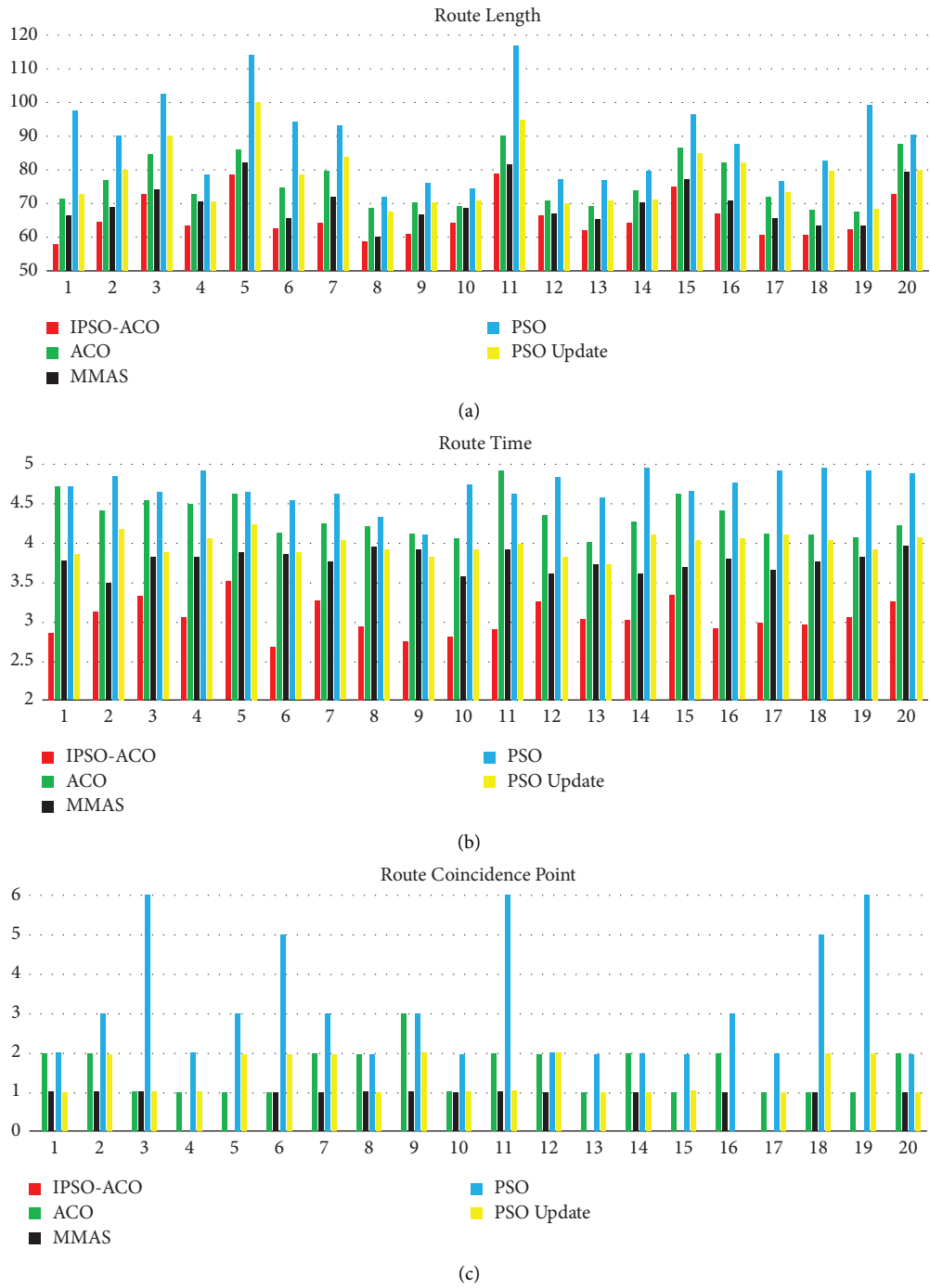


FIGURE 8: Intelligent algorithm simulation visualization results. (a) Intelligent algorithm dispatching route length; (b) intelligent algorithm dispatching route time; (c) intelligent algorithm route coincidence point.

TABLE 4: Average performance indicators of five intelligent algorithms.

Algorithm	Average route length (cm)	Average time (s)	Average coincidence point
IPSO-ACO	66.07	3.07	0
ACO	76.31	4.35	1.55
MMAS	70.16	3.79	0.7
PSO	80.10	4.73	3.15
PSO update	78.33	4.00	1.35

optimization algorithm, which can complete the safest and shortest energy dispatching route with the shortest time and the least energy consumption.

## 6. Conclusion and Future Work

This paper proposes an improved PSO-ACO algorithm combining PSO algorithm and ACO algorithm. It makes full use of the fast convergence ability of PSO algorithm and the robustness of ACO algorithm, which can improve the overall performance of energy dispatching, realize the safe, accurate and rapid energy dispatching, and effectively solve the problem of energy waste.

The improved PSO-ACO algorithm can obtain a better global optimal route in energy dispatching. Compared with ACO algorithm, MMAS algorithm, PSO algorithm, and PSO update algorithm, it has the shortest route length, less running time, no coincidence, and highest safety performance.

We verified the effectiveness and feasibility of the improved PSO-ACO algorithm through 20 sets of simulation experiments under different scenarios and proved that it is a successful algorithm that can be used to solve multi-objective optimization problems.

In the future, we can also consider other hybrid algorithms and combine the advantages of various algorithms to solve the multiobjective optimization problem of energy dispatching. In addition, we can continuously improve the complexity of energy dispatching scenarios, so that the optimization algorithm can quickly and accurately plan the optimal route in any working scenarios.

## Data Availability

The data used to support the findings of this study are included within the paper. All required models and parameters are listed in the paper.

## Conflicts of Interest

The authors declare that they have no conflicts of interest.

## Acknowledgments

This work was supported in part by the National Key Research and Development Program of China

(2020YFB1713300 and 2018AAA0101803); the National Natural Science Foundation of China (no. 52275480); and the Guizhou Province Higher Education Project (QJH KY (2020)005 and (2020)009).

## References

- [1] S. Koohi-Fayegh and M. A. Rosen, "A review of energy storage types, applications and recent developments," *Journal of Energy Storage*, vol. 27, Article ID 101047, 2020.
- [2] B. Huang, Y. Li, F. Zhan, Q. Sun, and H. Zhang, "A distributed robust economic dispatch strategy for integrated energy system considering ca," *IEEE Transactions on Industrial Informatics*, vol. 18, no. 2, pp. 880–890, 2022.
- [3] L. Uwineza, H. G. Kim, J. Kleissl, and C. K. Kim, "Technical control and optimal dispatch strategy for a hybrid energy system," *Energies*, vol. 15, no. 8, pp. 2744–2819, 2022.
- [4] X. Liu, S. Xie, C. Geng, J. Yin, G. Xiao, and H. Cao, "Optimal evolutionary dispatch for integrated community energy systems considering uncertainties of renewable energy sources and internal loads," *Energies*, vol. 14, no. 12, p. 3644, 2021.
- [5] H. E. Keshta, O. P. Malik, E. M. Saied, F. M. Bendary, and A. A. Ali, "Energy management system for two islanded interconnected micro-grids using advanced evolutionary algorithms," *Electric Power Systems Research*, vol. 192, Article ID 106958, 2021.
- [6] R. Hao, Z. Jiang, Q. Ai, Z. Yu, and Y. Zhu, "Hierarchical optimisation strategy in microgrid based on the consensus of multiagent system," *IET Generation, Transmission & Distribution*, vol. 12, no. 10, pp. 2444–2451, 2018.
- [7] J. Tan, "Energy management without iteration—a regional dispatch event-triggered algorithm for energy internet," *Frontiers in Energy Research*, vol. 10, pp. 1–14, 2022.
- [8] W. Dong, Q. Yang, X. Fang, and W. Ruan, "Adaptive optimal fuzzy logic based energy management in multi-energy microgrid considering operational uncertainties," *Applied Soft Computing*, vol. 98, Article ID 106882, 2021.
- [9] X. Li and K. W. Hedman, "Enhancing power system cybersecurity with systematic two-stage detection strategy," *IEEE Transactions on Power Systems*, vol. 35, no. 2, pp. 1549–1561, 2020.
- [10] M. N. Hindia, F. Qamar, M. B. Majed, T. Abd Rahman, and I. S. Amiri, "Enabling remote-control for the power substations over LTE-A networks," *Telecommunication Systems*, vol. 70, no. 1, pp. 37–53, 2019.
- [11] T. S. Lee, Y. T. Loong, and S. C. Tan, "A hybrid genetic-gravitational search algorithm for a multi-objective flow shop scheduling," *International Journal of Industrial Engineering Computations*, vol. 10, pp. 331–348, 2019.

- [12] W. Zhang and Y. Huang, "Using big data computing framework and parallelized PSO algorithm to construct the reservoir dispatching rule optimization," *Soft Computing*, vol. 24, no. 11, pp. 8113–8124, 2020.
- [13] H. I. Demir and C. Erden, "Dynamic integrated process planning, scheduling and due-date assignment using ant colony optimization," *Computers & Industrial Engineering*, vol. 149, Article ID 106799, 2020.
- [14] M. A. M. Shaheen, H. M. Hasanien, and A. Alkuhayli, "A novel hybrid GWO-PSO optimization technique for optimal reactive power dispatch problem solution," *Ain Shams Engineering Journal*, vol. 12, no. 1, pp. 621–630, 2021.
- [15] S. Chen, Z. Huang, and H. Guo, "An end-to-end deep learning method for dynamic job shop scheduling problem," *Machines*, vol. 10, no. 7, p. 573, 2022.
- [16] Z. Hongfeng, "Dynamic economic dispatch based on improved differential evolution algorithm," *Cluster Computing*, vol. 22, no. S4, pp. 8241–8248, 2019.
- [17] R. Shankar, A. Kumar, U. Raj, and K. Chatterjee, "Fruit fly algorithm-based automatic generation control of multiarea interconnected power system with FACTS and AC/DC links in deregulated power environment," *International Transactions on Electrical Energy Systems*, vol. 29, pp. 2690–2715, 2019.
- [18] A. L. Ara, N. Mohammad Shahi, and M. Nasir, "CHP economic dispatch considering p z to sustainable energy using self-regulating particle swarm optimization algorithm," *Iranian Journal of Science and Technology, Transactions of Electrical Engineering*, vol. 44, no. 3, pp. 1147–1164, 2020.
- [19] L. L. Li, J. L. Lou, M. L. Tseng, M. K. Lim, and R. R. Tan, "A hybrid dynamic economic environmental dispatch model for balancing operating costs and pollutant emissions in renewable energy: a novel improved mayfly algorithm," *Expert Systems with Applications*, vol. 203, Article ID 117411, 2022.
- [20] Z. G. Deng, J. H. Yang, C. I. Dong, M. Q. Xiang, Y. Qin, and Y. S. Sun, "Research on economic dispatch of integrated energy system based on improved krill swarm algorithm," *Energy Reports*, vol. 8, pp. 77–86, 2022.
- [21] L. Yu, X. Jin, Z. Li, Y. Xiong, and W. Huang, "An intelligent scheduling approach for electric power generation," *Chinese Journal of Electronics*, vol. 27, no. 6, pp. 1170–1175, 2018.
- [22] A. K. Sahoo, T. K. Panigrahi, G. Dhiman, K. K. Singh, and A. Singh, "Enhanced emperor penguin optimization algorithm for dynamic economic dispatch with renewable energy sources and microgrid," *Journal of Intelligent and Fuzzy Systems*, vol. 40, no. 5, pp. 9041–9058, 2021.
- [23] Y. Cao, T. Li, T. He, Y. Wei, M. Li, and F. Si, "Multiobjective load dispatch for coal fired power plants under renewable-energy accommodation based on a nondominated-sorting grey wolf optimizer algorithm," *Energies*, vol. 15, no. 8, p. 2915, 2022.
- [24] Y. Bo, Y. Xia, and W. Wei, "Ultra-short-term optimal dispatch for EH-IES considering uncertainty of delay in the distribution network," *International Journal of Electrical Power & Energy Systems*, vol. 141, Article ID 108214, 2022.
- [25] C. Paul, P. Kumar Roy, and V. Mukherjee, "Study of wind-solar based combined heat and power economic dispatch problem using quasi-oppositional-based whale optimization technique," *Optimal Control Applications and Methods*, 2021.
- [26] L. Lei, Y. Tan, G. Dahlenburg, W. Xiang, and K. Zheng, "Dynamic energy dispatch based on deep reinforcement learning in IoT-driven smart isolated microgrids," *IEEE Internet of Things Journal*, vol. 8, no. 10, pp. 7938–7953, 2021.
- [27] X. Chen, L. Huang, X. Zhang et al., "Robust optimal dispatching of wind fire energy storage system based on equilibrium optimization algorithm," *Frontiers in Energy Research*, vol. 9, pp. 1–7, 2021.
- [28] W. Wang, B. Sun, H. Li, Q. Sun, and R. Wennersten, "An improved min-max power dispatching method for integration of variable renewable energy," *Applied Energy*, vol. 276, Article ID 115430, 2020.
- [29] Y. Shang, Q. Fan, L. Shang, Z. Sun, and G. Xiao, "Modified genetic algorithm with simulated annealing applied to optimal load dispatch of the Three Gorges Hydropower Plant in China," *Hydrological Sciences Journal*, vol. 64, no. 9, pp. 1129–1139, 2019.
- [30] H. Qiu, W. Gu, X. Xu et al., "A historical-correlation-driven robust optimization approach for microgrid dispatch," *IEEE Transactions on Smart Grid*, vol. 12, no. 2, pp. 1135–1148, 2021.
- [31] M. Ellahi and G. Abbas, "A hybrid metaheuristic approach for the solution of renewables-incorporated economic dispatch problems," *IEEE Access*, vol. 8, pp. 127608–127621, 2020.
- [32] A. Zeng, S. Hao, J. Ning, Q. Xu, L. Jiang, and S. Lee, "Multiobjective optimized dispatching for integrated energy system based on hierarchical progressive parallel NSGA-II algorithm," *Mathematical Problems in Engineering*, vol. 2020, Article ID 6541782, 22 pages, 2020.
- [33] B. Li and J. Wang, "Economic dispatch methods for smart grid based on improved SPEA2 and improved NSGA2," *Frontiers in Energy Research*, vol. 9, pp. 1–11, 2021.
- [34] M. Wang, T. Zhang, P. Wang, and X. Chen, "An improved harmony search algorithm for solving day-ahead dispatch optimization problems of integrated energy systems considering time-series constraints," *Energy and Buildings*, vol. 229, Article ID 110477, 2020.
- [35] X. F. Song, Y. Zhang, D. W. Gong, and X. Y. Sun, "Feature selection using bare-bones particle swarm optimization with mutual information," *Pattern Recognition*, vol. 112, Article ID 107804, 2021.
- [36] X. F. Song, Y. Zhang, D. W. Gong, and X. Z. Gao, "A fast hybrid feature selection based on correlation-guided clustering and particle swarm optimization for high-dimensional data," *IEEE Transactions on Cybernetics*, vol. 52, no. 9, pp. 9573–9586, 2022.
- [37] H. C. Lu, H. Y. Tseng, and L. Yao, "Neutrino-like particle for particle swarm optimization," *International Journal of Intelligent Systems*, vol. 37, no. 1, pp. 859–913, 2022.
- [38] X. Ji, Y. Zhang, D. Gong, and X. Sun, "Dual-surrogate-assisted cooperative particle swarm optimization for expensive multimodal problems," *IEEE Transactions on Evolutionary Computation*, vol. 25, no. 4, pp. 794–808, 2021.
- [39] X. Ji, Y. Zhang, D. Gong, X. Sun, and Y. Guo, "Multisurrogate-assisted multitasking particle swarm optimization for expensive multimodal problems," *IEEE Transactions on Cybernetics*, vol. 11, pp. 1–15, 2021.
- [40] H. Ben Ammar, W. Ben Yahia, O. Ayadi, and F. Masmoudi, "Design of efficient multiobjective binary PSO algorithms for solving multi-item capacitated lot-sizing problem," *International Journal of Intelligent Systems*, vol. 37, no. 2, pp. 1723–1750, 2022.
- [41] R. Z. Zheng, Y. Zhang, and K. Yang, "A transfer learning-based particle swarm optimization algorithm for travelling salesman problem," *Journal of Computational Design and Engineering*, vol. 9, no. 3, pp. 933–948, 2022.



- [42] Y. Wang and Z. Han, "Ant colony optimization for traveling salesman problem based on parameters optimization," *Applied Soft Computing*, vol. 107, Article ID 107439, 2021.
- [43] J. P. Schmitt, R. S. Parpinelli, and F. Baldo, "Analysis of max-min ant system with local search applied to the asymmetric and dynamic travelling salesman problem with moving vehicle," *Lecture Notes in Computer Science*, pp. 202–218, 2019.
- [44] T. Li and L. Yaping, "An improved PSO algorithm for optimized material scheduling in emergency relief," *Mathematical Problems in Engineering*, vol. 2022, Article ID 5343521, 12 pages, 2022.
- [45] N. Chen and H. Zhou, "A comparison study of PSO with different update equations in solving economic dispatch problem," in *Proceedings of the 2020 39th Chinese Control Conference (CCC)*, pp. 6028–6032, Shenyang, China, July, 2020.